SUPPORTING INFORMATION

The detection sensitivity of commonly used singlet oxygen probes in aqueous environments

Tiago Entradas[a,b], Sarah Waldron[a], and Martin Volk[a,b]*

[a] Department of Chemistry, University of Liverpool, Crown Street, Liverpool L69 7ZD, United Kingdom

[b] Surface Science Research Centre, University of Liverpool, Abercromby Square, Liverpool L69 3BX, United Kingdom

* Corresponding author. E-mail address: m.volk@liverpool.ac.uk

Table of Contents

S1. Contamination of D_2O by H_2O

Even a small contamination by H_2O has a significant effect on the lifetime of $^1O_2$ in D_2O, which in turn affects the sensitivity of singlet oxygen probes. We used FTIR spectroscopy for measuring the H_2O content of our D_2O solvents. Fig. S1 shows two spectra taken for different D_2O batches as supplied, together with that of a sample of D_2O to which H_2O (5% v/v) had been added explicitly. As expected, the addition of H_2O leads to an increase of the band at 3400 cm^{-1}, arising from the OH stretch vibration and the band at 1460 cm^{-1}, arising from HOD, which is only visible as a shoulder on the D_2O association band at 1550 cm^{-1} in the spectra of the original D_2O solvent batches.

Comparison of the strength of the band at 3400 cm^{-1} with that of the 5% v/v H2O/D_2O sample showed that the different batches of D_2O which we used here contained 0.5-1% H_2O. The same conclusion can be drawn from the published extinction coefficient of the OH vibration band of H_2O [S1]. Since Rose Bengal stock solution was always prepared in H_2O, of which typically 10 μL were added to a 1 mL sample, a total H_2O content of 1.5-2% was present in our D_2O samples, and the H_2O content of the EtOH/D_2O could be estimated to be ~1.5%.

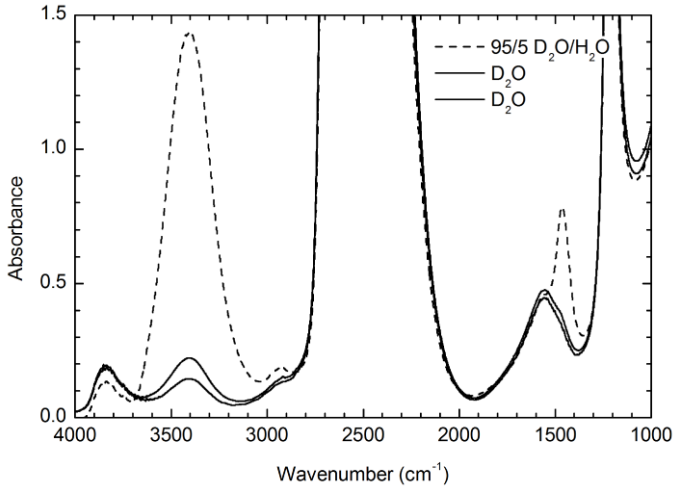

Fig. S1. FTIR spectra of different D_2O batches and of a sample of D_2O to which H_2O (5% v/v) had been added explicitly, measured in a 50 μm pathlength IR cell with CaF_2 windows, using a BioRad FTS-40 spectrometer.

S2. Derivation of Equation (5)

Since the lifetime of $^1O_2$ is very short compared to the experimental time scale (minutes) on which the probe concentration [P] changes, the steady-state concentration of $^1O_2$ at any given time *t* can be calculated by equating the rates of its photogeneration and its decay via solvent quenching or reaction with a probe molecule (all parameters as defined in the main text):

$$\frac{N_{\text{abs}}\Phi_{\text{RB}}}{VN_{\text{A}}} = \left[k_0 + (k_{\text{r}} + k_{\text{q}})[\text{P}]\right][^1\text{O}_2]_{\text{ss}} \qquad \text{(S1) = (3)}$$

Using this steady-state concentration of $^1O_2$ from Eq. (S1) yields the rate of bleach of probe P due to reaction with $^1O_2$:

$$\frac{d[\text{P}]}{dt} = -k_{\text{r}}[\text{P}][^1\text{O}_2] = -k_{\text{r}}[\text{P}]\frac{N_{abs}\Phi_{RB}}{VN_A\left[k_0 + (k_{\text{r}} + k_{\text{q}})[\text{P}]\right]} \qquad \text{(S2) = (4)}$$

In this equation, the probe concentration [P] can be replaced by the (time-dependent) absorbance $A = \varepsilon d[\text{P}]$:

$$\frac{dA}{dt} = \varepsilon d\frac{d[\text{P}]}{dt} = -k_r A\frac{N_{\text{abs}}\Phi_{\text{RB}}}{VN_{\text{A}}(k_0 + (k_{\text{r}} + k_{\text{q}})\frac{A}{\varepsilon d})} = -A\frac{\varepsilon dN_{\text{abs}}\Phi_{\text{RB}}}{VN_{\text{A}}(\varepsilon d\frac{k_0}{k_{\text{r}}} + \frac{k_{\text{r}} + k_{\text{q}}}{k_{\text{r}}}A)} = -\frac{A}{C_1(C_2 + C_3A)} \qquad \text{(S3)}$$

where $C_1 = \frac{VN_{\text{A}}}{\varepsilon dN_{\text{abs}}\Phi_{\text{RB}}}$, $C_2 = \frac{\varepsilon dk_0}{k_{\text{r}}}$, and $C_3 = \frac{k_{\text{r}} + k_{\text{q}}}{k_{\text{r}}}$

Eq. (S3) yields the following differential equation:

$$\frac{C_1(C_2 + C_3A)}{A}dA + dt = 0 \qquad \text{(S4)}$$

Eq. (S4) can be solved by direct integration:

$$0 = \int_{A_0}^{A(t)}\frac{C_1(C_2 + C_3A)}{A}dA + \int_0^t dt = C_1C_2\ln\frac{A(t)}{A_0} + C_1C_3(A(t) - A_0) + t \qquad \text{(S5)}$$

Eq. (S5) can be re-arranged to yield Eq. (5):

$$t = C_1\left(C_2\ln\frac{A_0}{A(t)} + C_3[A_0 - A(t)]\right) \qquad \text{(S6) = (5)}$$

S3. Photostability of Singlet Oxygen Sensitizer and Probes

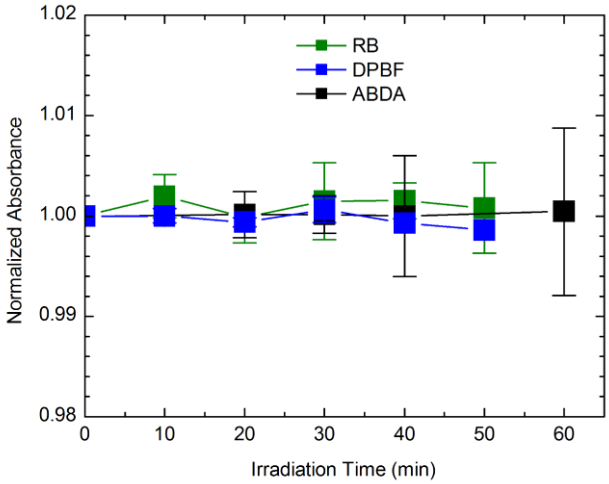

Fig. S2. Stability of RB, DPBF and ABDA upon irradiation when used separately. Shown here is the absorbance of RB in H_2O at 552 nm (green), DPBF in 50/50 (v/v) EtOH/H_2O at 411 nm (blue), and ABDA in D_2O at 400 nm (black), during irradiation with 0.14 mW cw laser light at 532 nm, normalized to the absorbance at the start of the irradiation, averaged over several repeat experiments; the error bars were calculated from the standard deviations for the individual experiments.

S4. Data Fits Using Eq. (5)

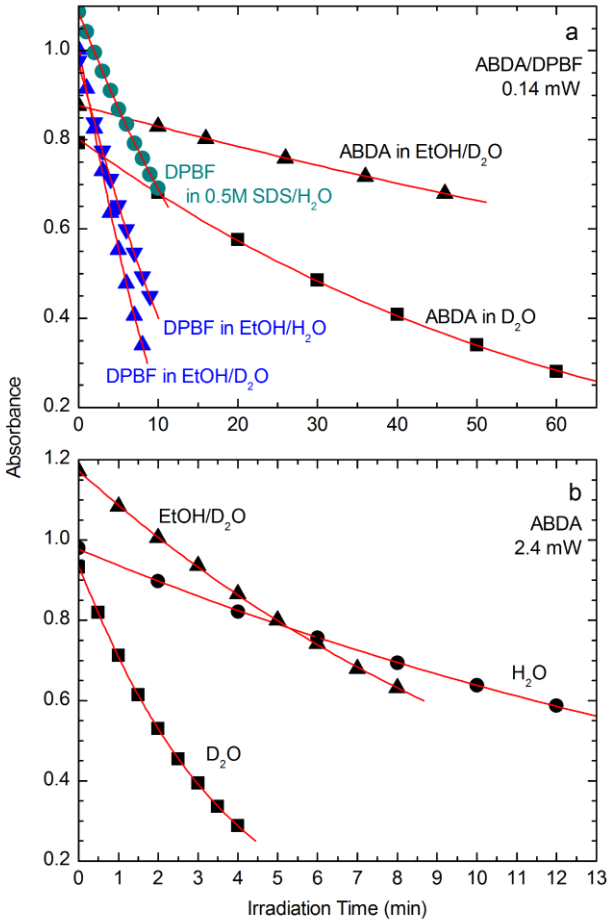

Fig. S3. Example results of the photobleaching of ABDA (black) and DPBF (blue, dark cyan) in different solvents upon irradiation with 0.14 mW (a) or 2.4 mW (b) cw laser light at 532 nm in the presence of photosensitizer RB; shown here is the absorbance at 398-400 nm (ABDA) or 410-412 nm (DPBF); the concentration of RB (~2 – 4 μM), and hence the amount of photogenerated $^1O_2$, varied between the different curves, so that they are quantitatively not fully comparable; mixed solvents are 50/50 (v/v) mixtures. The red lines are fits of the data to Eq. (5), where Parameter C_1 was calculated from the experimental parameters, the probe extinction coefficient (Table 1) and the $^1O_2$ quantum yield of RB, Parameter C_3 was set to 1.2 (ABDA) or 1 (DPBF), as justified in the main text, and C_2 and A_0 were the free fit parameters. It should be noted that, unlike Fig. 4, Fig. S3 shows the time-dependent absorbance measured in individual experiments without any normalization, as required for application of Eq. (5).

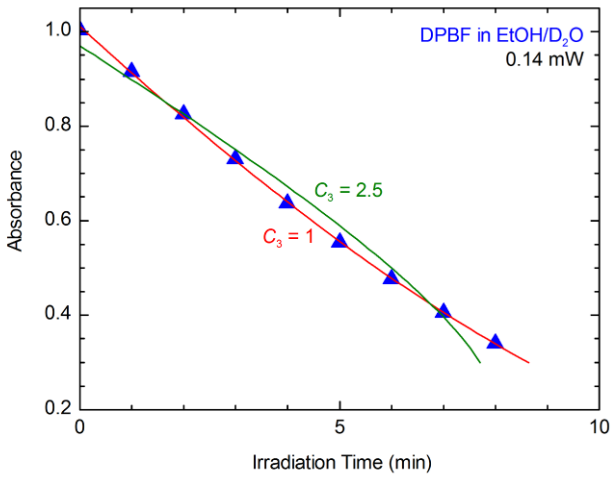

Fig. S4. Fits of the example results of the photobleaching of DPBF in 50/50 (v/v) EtOH/D_2O upon irradiation with 0.14 mW cw laser light at 532 nm in the presence of photosensitizer RB; shown here is the absorbance at 410-412 nm (DPBF). The red line is the fit of the data to Eq. (5) with Parameter C_3 set to 1, the green line the fit with C_3 = 2.5. Parameter C_1 was calculated from the experimental parameters, the probe extinction coefficient (Table 1) and the $^1O_2$ quantum yield of RB, as justified in the main text, and C_2 and A_0 were the free fit parameters.

Table S1

Rate constant k_r for deactivation of $^1O_2$ by a chemical reaction with a $^1O_2$ probe and resulting $^1O_2$ sensitivity Φ_P at probe concentrations corresponding to a maximum absorbance of 1, for ABDA and DPBF in different solvents, obtained from the data using fits to Eq. (5) under the assumption of different values of parameter $C_3 = (k_r + k_q)/k_r$. The highlighted results are those reported in the main text.

$^1O_2$ probe	solvent	C_3						
		1	1.1	1.2	1.35	1.6	2	2.5
		k_r (10^7 $M^{-1}s^{-1}$)						
ABDA[a]	H_2O	5.60	5.60	5.61	5.63	5.65	5.68	5.73
	D_2O	3.89	3.89	3.92	3.98	4.07	4.24	4.47
	EtOH/D_2O[b]	2.75	2.77	2.78	2.79	2.82	2.87	2.93
DPBF	EtOH/H_2O[b]	283	302	323	361	450	751	2600[c]
	EtOH/D_2O[b]	231	272	332	493	2900[c]	-451[d]	-182[d]
	0.1 M SDS/H_2O	230	236	243	253	274	314	386
	0.5 M SDS/H_2O	177	185	194	210	245	340	768
		Φ_P						
ABDA[a]	H_2O	0.0192	0.0192	0.0192	0.0192	0.0192	0.0191	0.0191
	D_2O[e]	0.183	0.180	0.178	0.175	0.171	0.164	0.157
	EtOH/D_2O[b,e]	0.0501	0.0501	0.0500	0.0499	0.0498	0.0495	0.0492
DPBF	EtOH/H_2O[b]	0.449	0.444	0.439	0.432	0.421	0.406	0.380
	EtOH/D_2O[b,e]	0.722	0.701	0.681	0.653	0.613	0.555	0.498
	0.1 M SDS/H_2O	0.308	0.304	0.300	0.295	0.287	0.275	0.261
	0.5 M SDS/H_2O	0.299	0.300	0.301	0.302	0.305	0.311	0.329

[a] ABDA samples contained 1% (v/v) DMSO.
[b] 50/50 (v/v).
[c] this result for k_r is unphysical since it is significantly larger than the maximum diffusion-limited reaction rate constant, compare the Discussion section of the main text. It is included here only for the sake of completeness.
[d] for large values of C_3, the fits of the DPBF data in EtOH/D_2O do not result in satisfactory results, see Fig. S4, and yield a negative rate constant; this unphysical result is based on the fact that for $C_3 > 2$, i.e. $k_q > k_r$, the maximum theoretically possible value of Φ_P is 0.5, which is significantly smaller than the experimentally observed value as analyzed by Eq. (2). As discussed in the main text, the literature confirms that for DPBF $k_q < 0.1\ k_r$, so this physically impossible result for k_r is reported here only for the sake of completeness.
[e] assuming neat solvents, *i.e.* no contamination by H_2O.

S5. Two-Pseudophase Model for Reactions of $^1O_2$ in Micellar Solution

Lee and Rodgers developed a two-pseudophase model for describing the reaction of $^1O_2$ with a quencher in a microheterogeneous environment [S2,S3], which has been used widely for micellar solutions, nanocapsules and microemulsions [S4–S6]. Scheme S1 shows schematically the relevant reactions describing the change of the micellar concentration of oxygen (in either the ground or the singlet state), which include the transfer from the aqueous to the micellar phase and vice versa, with first order rate constants k_{in} and k_{out}, respectively, and the intrinsic decay of $^1O_2$ due to solvent quenching with rate constants k_0 and $k_{0,m}$ in the two phases, respectively. Finally, $^1O_2$ can also react with DPBF, which is found exclusively in the micellar environment, with a rate constant $k_{r,m}$ (here, physical quenching of $^1O_2$ by DPBF is neglected, as justified in section 3.3).

Scheme S1

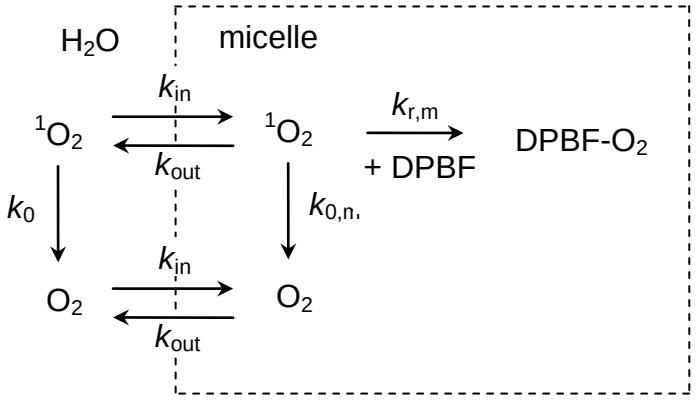

Diffusion of O_2 (or $^1O_2$) into and out of micelles has been shown to proceed on the 10-100 ns time scale [S7,S8], essentially limited by diffusion between the micelles: with a diffusion constant of 1.9×10^{-5} cm^2/s [S9], O_2 requires ~10 ns to diffuse over a length scale of 10 nm, which corresponds to the average intermicellar distance at 0.1 M SDS. Thus, transfer between the phases is much faster than the intrinsic decay of $^1O_2$ even in H_2O, where $^1O_2$ has a lifetime of ~4 μs, resulting in fast equilibration of molecular oxygen and $^1O_2$ between the aqueous phase and the micelles. In equilibrium the concentration of $^1O_2$ inside the micelle, $[^1O_2]_{mic}$, is larger than the concentration in the aqueous phase, $[^1O_2]_{aq}$, by a factor $K = [^1O_2]_{mic}/[^1O_2]_{aq} = 2.9$, as shown by the dependence of the lifetime of $^1O_2$ on the concentration of SDS [S2,S8], which is equal to the partitioning of ground state oxygen, as measured via the oxygen solubility in SDS solutions using a manometric technique [S10].

The concentration of micelles (1.5 mM at 0.1 M SDS, given a critical micelle concentration, *cmc*, of ~7.5 mM [S11-S13] and an aggregation number, n_m, of ~63 [S13-S15]) is significantly larger than the concentration of DPBF (~0.05 mM), so that most micelles do not contain DPBF and there are virtually no micelles containing more than one DPBF molecule. The intrinsic lifetime of $^1O_2$ inside micelles in the absence of an additional quencher was found to be 20 μs [S2].

Given the fast equilibration between the two phases, $[^1O_2]_{mic} = K\,[^1O_2]_{aq}$ at all times and the total concentration is given by $[^1O_2] = (1\text{-}f)\,[^1O_2]_{aq} + f\,[^1O_2]_{mic} = (1 - f + f\,K)\,[^1O_2]_{aq}$, where f denotes the volume fraction of the micellar phase, which can be calculated using the partial molar volume of SDS, $v_{SDS} = 0.246$ dm^3/mol [S16]: $f = ([SDS] - cmc) \times v_{SDS}$. Scheme S1 then predicts an overall rate of decay of $^1O_2$ given by

$$
\begin{aligned}
-\frac{\mathrm{d}[^1O_2]}{\mathrm{d}t} &= (1-f)\frac{\mathrm{d}[^1O_2]_{aq}}{\mathrm{d}t} + f\frac{\mathrm{d}[^1O_2]_{mic}}{\mathrm{d}t} \\
&= (1-f)\,k_0[^1O_2]_{aq} + f\,k_{0,m}[^1O_2]_{mic} + f\,k_{r,m}[^1O_2]_{mic}\,[DPBF]_{mic} \\
&= \left((1-f)\,k_0 + f\,k_{0,m}\,K\right)[^1O_2]_{aq} + f\,k_{r,m}\,K\,[^1O_2]_{aq}\,[DPBF]/f \\
&= \frac{\left((1-f)\,k_0 + f\,k_{0,m}\,K\right)}{(1-f)+f\,K}[^1O_2] + \frac{k_{r,m}\,K}{(1-f)+f\,K}[^1O_2]\,[DPBF]
\end{aligned}
\qquad \text{(S7)}
$$

Here, $[DPBF]_{mic}$ denotes the concentration of DPBF in the micellar phase, $[DPBF]_{mic} = [DPBF]/f$, with [DPBF] denoting the total concentration of DPBF.

Using $k_0 = 1/(4.2\ \mu s)$ (see section 3.2 of the main text), $k_{0,m} = 1/(20\ \mu s)$ (see above), equation (S7) predicts intrinsic $^1O_2$ lifetimes (in the absence of DPBF) of 4.4 μs and 5.4 μs for solutions with 0.1 M and 0.5 M SDS, respectively, which is in good agreement with the experimentally reported values, compare section 3.2. Moreover, the effective rate constant k_r is shown to be given by [S3,S5]

$$
k_r = k_{r,m}\,\frac{K}{K\,f + (1-f)} \qquad \text{(S8) = (7).}
$$

References

[S1] S.Y. Venyaminov, F.G. Prendergast, Water (H_2O and D_2O) Molar Absorptivity in the 1000-4000 cm^{-1} Range and Quantitative Infrared Spectroscopy of Aqueous Solutions, Anal. Biochem. 248 (1997) 234-245, https://doi.org/10.1006/abio.1997.2136.

[S2] P.C. Lee, M.A.J. Rodgers, Singlet Molecular Oxygen in Micellar Systems. 1. Distribution Equilibria between Hydrophobic and Hydrophilic Compartments, J. Phys. Chem. 87 (1983) 4894-4898, https://doi.org/10.1021/j150642a027.

[S3] M.A.J. Rodgers, P.C. Lee, Singlet Molecular Oxygen in Micellar Systems. 2. Quenching Behaviour in AOT Reverse Micelles, J. Phys. Chem. 88 (1984) 3480-3484, https://doi.org/10.1021/j150660a021.

[S4] C.D. Borsarelli, E.N. Durantini, N.A. Garcia, Singlet Molecular Oxygen-Mediated Photooxidation of Nitrophenolic Compounds in Water-in-Oil Microemulsions. A Kinetic Study, J. Chem. Soc., Perkin Trans. 2 (1996) 2009-2013, https://doi.org/10.1039/p29960002009.

[S5] A. Sivery, A. Barras, R. Boukherroub, C. Pierlot, J.M. Aubry, F. Anquez, E. Courtade, Production Rate and Reactivity of Singlet Oxygen $^1O_2(^1\Delta_g)$ Directly Photoactivated at 1270 nm in Lipid Nanocapsules Dispersed in Water, J. Phys. Chem. C 118 (2014) 2885-2893, https://doi.org/10.1021/jp412497k.

[S6] L.A. Martinez, C.G. Martinez, B.B. Klopotek, J. Lang, A. Neuner, A.M. Braun, E. Oliveros, Nonradiative and Radiative Deactivation of Singlet Oxygen ($O_2(a^1\Delta_g)$) in Micellar Media and Microemulsions, J. Photochem. Photobiol., B 58 (2000) 94-107, https://doi.org/10.1016/S1011-1344(00)00109-3.

[S7] N.J. Turro, M. Aikawa, A. Yekta, Dynamics of Molecular Oxygen in Micellar Solutions, Chem. Phys. Lett. 64 (1979) 473-478, https://doi.org/10.1016/0009-2614(79)80225-0.

[S8] I.B.C. Matheson, R. Massoudi, Photophysical and Photosensitized Generation of Singlet Molecular Oxygen ($^1\Delta_g$) in Micellar Solutions at Elevated Pressures. Measurement of Single Molecular Oxygen Solvent to Micelle Transfer Rates via Both Molecular Diffusion and Energy Transfer, J. Am. Chem. Soc. 102 (1980) 1942-1948, https://doi.org/10.1021/ja00526a031.

[S9] P. Han, D.M. Bartels, Temperature Dependence of Oxygen Diffusion in H_2O and D_2O, J. Phys. Chem. 100 (1996) 5597-5602, https://doi.org/10.1021/jp952903y.

[S10] I.B.C. Matheson, A.D. King, Solubility of Gases in Micellar Solutions, J. Colloid Interface Sci. 66 (1978) 464-469, https://doi.org/10.1016/0021-9797(78)90066-8.

[S11] N.J. Turro, P.C.C. Lee, Perfluorinated "Mini" Micelles: Energy Transfer from Benzophenone and Determination of Aggregation Number, J. Phys. Chem. 86 (1982) 3367-3371, https://doi.org/10.1021/j100214a020.

[S12] R.J. Williams, J.N. Phillips, K.J. Mysels, The Critical Micelle Concentration of Sodium Lauryl Sulphate at 25^{o}C, Trans. Faraday Soc. 51 (1955) 728-737, https://doi.org/10.1039/tf9555100728.

[S13] F. Reiss-Husson, V. Luzzati, The Structure of the Micellar Solutions of Some Amphiphilic Compounds in Pure Water as Determined by Absolute Small-Angle X-Ray Scattering Techniques, J. Phys. Chem. 68 (1964) 3504-3511, https://doi.org/10.1021/j100794a011.

[S14] N.J. Turro, A. Yekta, Luminescent Probes for Detergent Solutions. A Simple Procedure for Determination of the Mean Aggregation Number of Micelles, J. Am. Chem. Soc. 100 (1978) 5951-5952, https://doi.org/10.1021/ja00486a062.

[S15] H. Coll, Study of Ionic Surfactants by Membrane Osmometry, J. Phys. Chem. 74 (1970) 520-528, https://doi.org/10.1021/j100698a008.

[S16] J.M. Corkill, J.F. Goodman, T. Walker, Partial Molar Volumes of Surface-Active Agents in Aqueous Solution, Trans. Faraday Soc. 63 (1967) 768-772, https://doi.org/10.1039/tf9676300768.